

Received: 2017.01.18  
Accepted: 2017.02.27  
Published: 2017.04.05

# Effects of Cone-Shaped Bend Inlet Cannulas of an Axial Blood Pump on Thrombus Formation: An Experiment and Simulation Study

State Key Laboratory of Cardiovascular Disease, Fuwai Hospital, Beijing, P.R. China

Authors' Contribution:  
Study Design A  
Data Collection B  
Statistical Analysis C  
Data Interpretation D  
Manuscript Preparation E  
Literature Search F  
Funds Collection G

ACEF **Guangmao Liu**  
BD **Jianye Zhou**  
A **Hansong Sun**  
C **Yan Zhang**  
B **Haibo Chen**  
DG **Shengshou Hu**

**Corresponding Author:** Jianye Zhou, e-mail: [zhoujianye@fuwaihospital.org](mailto:zhoujianye@fuwaihospital.org)

**Source of support:** The National Natural Science Foundation of China (81550050 and 51236001) supported this research

**Background:** Cannula shape and connection style influence the risk of thrombus formation in the blood pump by varying the blood flow characteristics inside the pump. Inlet cannulas should be designed based on the need for anatomical fit and reducing the risk of thrombus generation in the blood pump. The effects on thrombus formation of the cone-shaped bend inlet cannulas of axial blood pumps should be studied.





**Material/Methods:** The cannulas were designed as cone-shaped, with 1 bent section connecting 2 straight sections. Both the silicone tube and novel cone-shaped cannula were simulated for comparison. The flow fields of a blood pump with inlet cannula were simulated by computational fluid dynamics (CFD) at flows of 2.0, 2.5, and 3.0 liters per minute (lpm), with pump rotational speeds of 7500, 8000, and 8500 rpm, respectively. Then, 6 two-dimensional (2D) particle image velocimetry (PIV) tests were conducted and the velocity distributions were analyzed.

**Results:** A low-velocity region was located inside the pump entrance when a soft silicone tube was used. At 8500 rpm and 3.0 lpm working condition, the minimum velocity inside the pump with cone-shaped cannulas was  $2.5 \times 10^{-1}$  m/s. The cone-shaped cannulas eliminated the low-velocity region inside the pump. Both CFD and PIV results showed that the low-velocity region did not spread to the entrance of the blood pump within the flow range from 2.0 lpm to 7.0 lpm.

**Conclusions:** The designed cone-shaped bent cannulas can eliminate the low-velocity region inside the blood pump and reduce the risk of thrombus formation in the blood pump.

**MeSH Keywords:** **Assist Devices • Hemodynamics • Numerical Analysis, Computer-Assisted • Thrombosis**

**Full-text PDF:** <http://www.medscimonit.com/abstract/index/idArt/903421>

 1953  —  6  21



## Background

Axial blood pumps have been widely used to assist the circulation of patients with heart failure and have been proven effective [1–5]. Reducing the risks of thrombosis and hemolysis is the emphasis of axial blood pump research. Generally, adverse high shear stress or flow separation cannot cause hemolysis in the inlet cannulas [6]. However, the flow fields in the cannulas are closely related to the thrombosis property of the axial blood pump [7]. Cannulas are an important component of adverse events such as thrombus formation in patients with pumps by varying the flow status of the blood that enters and leaves the pump.

Cannula shape, design parameters, and connection style directly influence the dynamics of the interior blood flow and the pump itself [7–9]. Related studies have identified that the blood pump inlet cannula influences the rate of cerebrovascular adverse events [10–12]. The blood pump inlet cannula is usually inserted into the left ventricle (LV) apex [13,14]. Javid Fatullayev's study revealed that the positioning of the inflow cannula and the size of the pump pocket were shown to putatively contribute to thrombosis [15]. Therefore, cannulas directly influence thrombus formation during clinical blood pumping. Appropriately designed inlet cannulas would improve the anatomical fitting of the cannula and pump.

Computational fluid dynamics (CFD) technology has been successfully used to design blood pumps and analyze their blood flow [16,17]. Particle image velocimetry (PIV) can test transient flow velocity indirectly by testing the flow displacement of the tracer particle in a brief time period. PIV technology has

been used to visualize the flow within blood pumps for more than 10 years [10,18].

An extracorporeal axial blood pump called LAP23 [19] with a severely bent medical silicone tube was used in an animal experiment, as shown in Figure 1A. Figure 1B displays thrombi generated at the pump entrance inner wall in the animal experiment. We analyzed the causes of thrombi generation in animal experiments using CFDs and designed specialized inlet cannulas for the axial blood pump. The effects of the designed cone-shaped bend inlet cannulas of axial blood pumps on thrombus formation were studied by CFD and PIV technology.

## Material and Methods

### Design

The axial blood pump was connected to the patient's circulation system with inlet and outlet cannulas. The inlet cannula tip was connected to the apex of the LV, and it extended out of the patient's body to connect to the blood pump. The blood pump was placed extracorporeally and was connected to the ascending or descending aorta with the outlet cannula. Figure 2 illustrates the design of the inlet cannulas. The length and bend angle of the cannulas were designed based on the connection mode of the LAP23. The bends of the cannulas did not vary from case to case because the outlet cannula can be sutured to the aorta from the ascending aorta to the descending aorta. Moreover, the cone-shaped structure was designed with regard to both improvements in the blood flow status and decreases in vessel damage when the outlet cannula is fitted

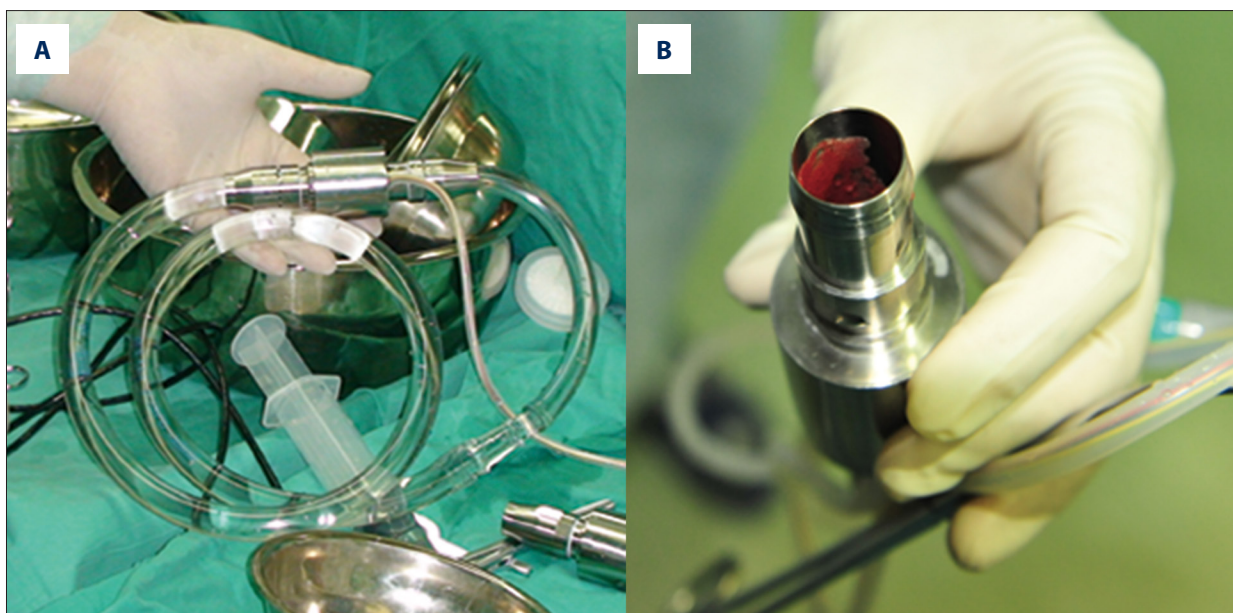


**Figure 1.** (A) LAP23 with a medical silicone tube. (B) Thrombus in the LAP23 after an animal experiment using a medical silicone tube.

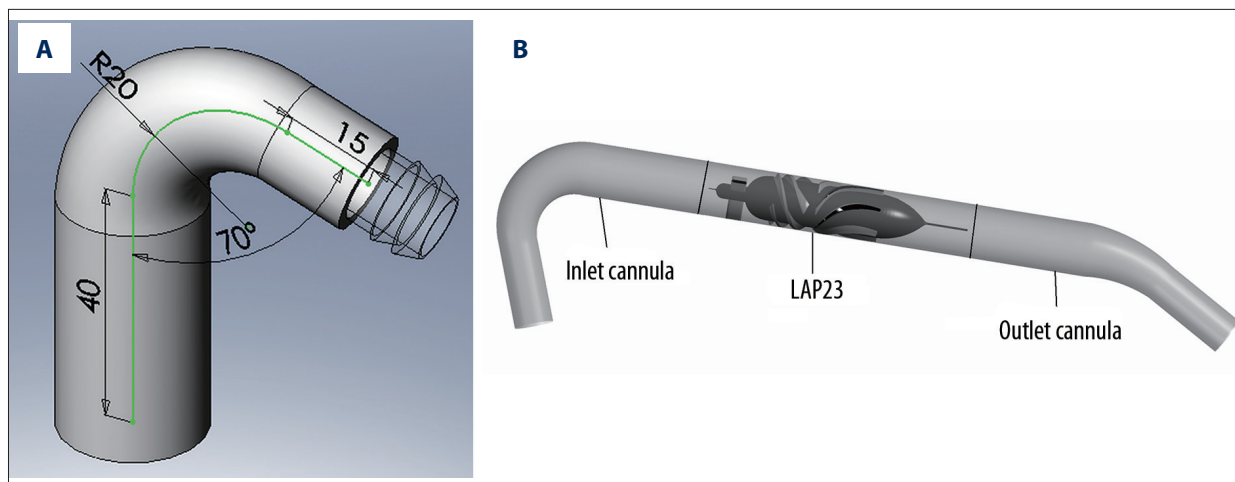


**Figure 2.** (A) Geometry of the inlet cannulas; (B) LAP23 with inlet and outlet cannulas.

to the ascending or descending aorta. The bent angle of the LAP23 inlet cannula fitting for patients was from 60° to 80° based on 5 clinical trials of the LAP23. Thus, the inlet cannula was designed as cone-shaped with a 70° bend angle. The inner diameters of the inlet cannulas gradually changed from 20 mm to 12.7 mm. The inlet cannulas contained 2 straight sections and 1 bent section. The curvature radius of the bent section of the inlet cannula was 20 mm. The cone-shaped inlet cannula was made with medical silicone tube, and steel wire was embedded in the silicone tube to maintain the cannula's structure.

### Simulation

A commercial CFD package solver (CFX 12.1, ANSYS, Inc., Canonsburg, PA, USA) of the Reynolds-averaged Navier-Stokes equations was used to simulate the flow of the blood pump with the soft medical silicone tube (like that in the animal experiment) and cone-shaped bent cannulas, respectively. A grid convergence study was completed to evaluate the influence of the number of grid elements on the accuracy of the CFD results and the computational convergence times. The O grids generated at the zones near the pump blades and the more refined grids near the walls were specified to gain the boundary layer properties. A static pressure of 10 mmHg and temperature of 37°C were set at the entrance of the inlet cannula. Flow rates of 2.0 lpm, 2.5 lpm, and 3.0 lpm were set in the outlet region of the outlet cannula. The speeds of the rotor impeller in the blood pump were 7500, 8000, and 8500 rpm. The Reynolds-averaged Navier-Stokes equations were defined as follows:

$$\begin{cases} \frac{\partial \bar{u}_i}{\partial x_i} = 0 \\ \frac{\partial(\rho \bar{u}_i)}{\partial t} + \frac{\partial(\rho \bar{u}_i \bar{u}_j)}{\partial x_j} = -\frac{\partial \bar{p}}{\partial x_i} + \frac{\partial}{\partial x_j} \mu \frac{\partial \bar{u}_i}{\partial x_j} - \overline{\rho u'_i u'_j} + \bar{f}_i \end{cases} \quad (1)$$

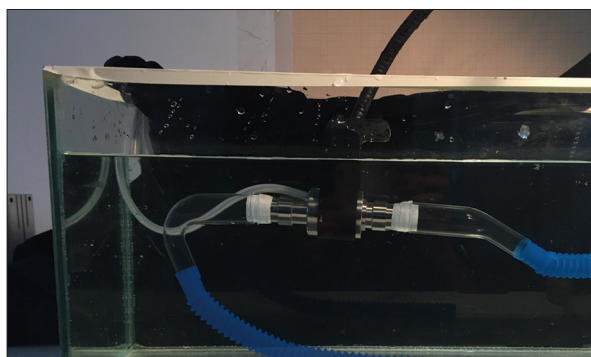


**Figure 3.** PIV test loop.

Where  $u_i$  (m/s) is the velocity,  $x_i$  (m) is the displacement,  $\rho$  is density,  $p$  (pa) is the pressure,  $\mu$  (m<sup>2</sup>/s) is dynamic viscosity, and  $f_i$  (N/m<sup>2</sup>) is mass force.

The blood was treated as Newtonian in most computational regions where the shear rate was greater than 100/s in this simulation [20]. The incompressible blood fluid parameters are listed as: density ( $\rho$ )=1055 kg/m<sup>3</sup> and dynamic viscosity=3.5×10<sup>-3</sup> Pa/s. The Reynolds number was then calculated as approximately 2×10<sup>5</sup>; thus, the turbulent flow dominated the entire flow status. In this study, the  $k$  (turbulent kinetic energy) –  $\epsilon$  (viscous dissipation) turbulence model was chosen.

### PIV

We designed the 2D PIV system to test the flow distribution in the inlet cannulas. The PIV systems were purchased from Beijing Cube Field Sci-Tech Development Co. Ltd. The tested inlet and outlet cannulas were constructed of hyaline glass. The entire experimental loop was placed into a hyaline container filled with water to alleviate the refraction of the circular cannula (Figure 3). The experiments were performed at a rotational speed of 7500±50 rpm, with a flow rate of 2.0 lpm;

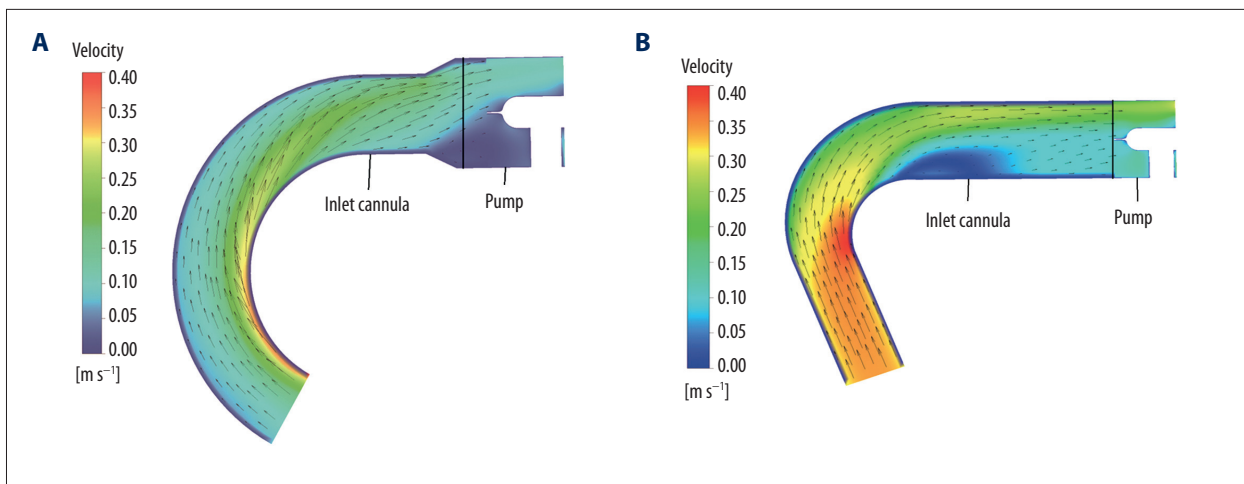


**Figure 4.** The flow field prior to the pump entrance at 8500 rpm and 3.0 lpm. (A) With the same soft silicone tube showed as Figure 1A; (B) With the cone-shaped inlet cannula.

8000±50 rpm with a flow rate of 2.5 lpm; and 8500±50 rpm with a flow rate of 3.0 lpm. The specific gravity and dynamic viscosity of the mixture consisting of water and glycerine were 1055 kg/m<sup>3</sup> and 3.5 kg/m/s, respectively, simulating the property of blood. Each of the 6 tests measured and calculated 100 instantaneous flow fields. The PIV results were calculated by averaging the 100 instantaneous flow fields.

## Results

Figure 4 illustrates the velocity distribution along the median plane of the inlet cannulas and pump entrance at 8500 rpm and 3.0 lpm. Figure 4A shows the flow stagnation region that existed inside the pump. The minimum velocity in the flow stagnation region was  $3.2 \times 10^{-3}$  m/s. Figure 4B shows that the velocity inside the blood pump was approximately  $2.5 \times 10^{-1}$  m/s, with no low-velocity region in the pump.

Figure 5 illustrates the velocity distribution along the median plane of the inlet cannula. PIV revealed higher local velocities than CFD. CFD and PIV showed similar flow following the inlet cannulas. Figure 5A and 5B show that the velocity in the inlet cannula decreases gradually along the cannula axial direction as the diameter of the inlet cannula gradually increased. In addition, a low-velocity region existed around the inner side after the bent section. Figure 5C–5F show that low-velocity region located in the inlet cannula was enlarged when the flow rate increased from 2.0 lpm to 3.0 lpm. The minimum velocity in the inlet cannula low-velocity region increased from  $5.0 \times 10^{-2}$  m/s to  $9.0 \times 10^{-2}$  m/s.

Figure 6 illustrates the calculated velocity distribution along the median plane of the cone-shaped inlet cannula at flow rate of 4.0 lpm, 5.0 lpm, 6.0 lpm, and 7.0 lpm. CFD results

showed favorable flow following the inlet cannulas when the blood pump LAP23 worked within the flow rate range from 4.0 lpm to 7.0 lpm.

## Discussion

The CFD results showed that a flow stagnation region existed inside the pump where the thrombi were generated in the animal experiment and explained why the thrombi were generated at the blood pump inner wall. The simulation showed a low-velocity region existed after the bent section of the cone-shaped inlet cannula, but disappeared before the blood flow into the entrance of the blood pump. The straight section of the cone-shaped inlet cannula connecting the blood pump was long enough to eliminate the stagnant flow inside the entrance of the blood pump. The gradually changed inner radius of the cone-shaped cannula avoided the stagnant velocity region caused by a suddenly changed flow area. The results show that the cone-shaped bent inlet cannula reduced the risk of thrombus formation in the blood pump. The study shows that low-velocity flow or stagnant flow regions are located at the location of the thrombus within the inlet cannula, as shown in Fraser' study [6] on drainage cannulas. Compared to the flow visualization experiment conducted by Medvitz [18] and Curtis [21], this PIV can give clearer results on velocity distribution in the tested cannula.

LAP23 is a short-term, extracorporeal blood pump. The 20-mm entrance diameter of the blood pump can cause severe damage to the LV because its large diameter requires a large anastomosis on the LV. Moreover, the 20-mm exit diameter of the blood pump is too large to be sutured to the ascending or descending aorta. The cone-shaped structure was selected to change the diameter of the anastomosis section

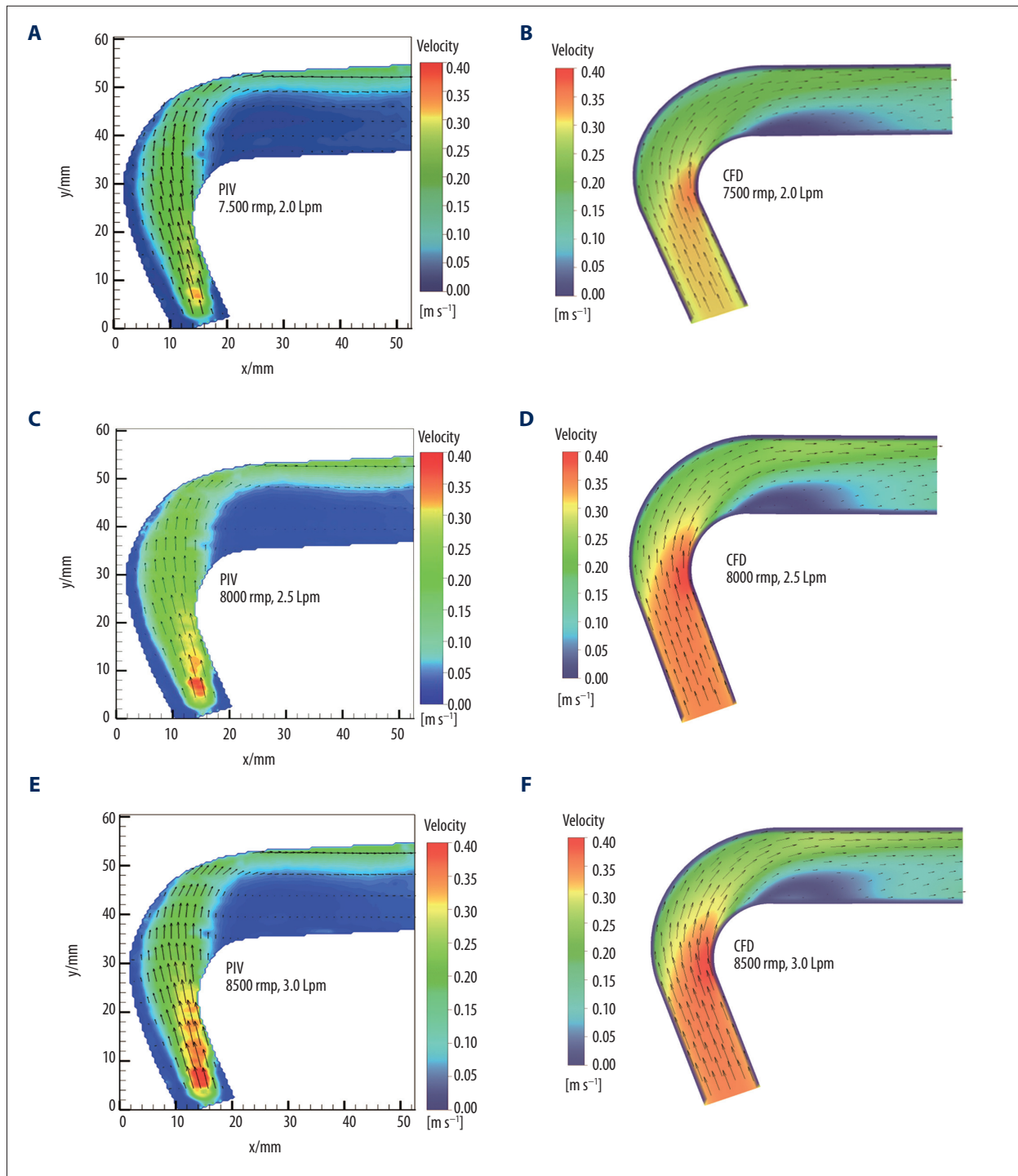


**Figure 5.** The flow field in the inlet cannula. (A) CFD results at 7500 rpm and 2.0 lpm; (B) PIV results at 7500 rpm and 2.0 lpm; (C) CFD results at 8000 rpm and 2.5 lpm; (D) PIV results at 8000 rpm and 2.5 lpm; (E) CFD results at 8500 rpm and 3.0 lpm; (F) PIV results at 8500 rpm and 3.0 lpm.

from 20 mm to 12.7 mm by smoothly reducing the flow passage area to avoid the flow separation caused by a sudden velocity change. The specific angle was selected according to the placement of the heart, the blood pump, and the thoracic

aorta. The velocity distribution results showed that the larger bend angle of 70° in the inlet cannula rapidly altered the flow direction, which led to a velocity gradient. This altered blood flow caused a low-velocity region within the straight section

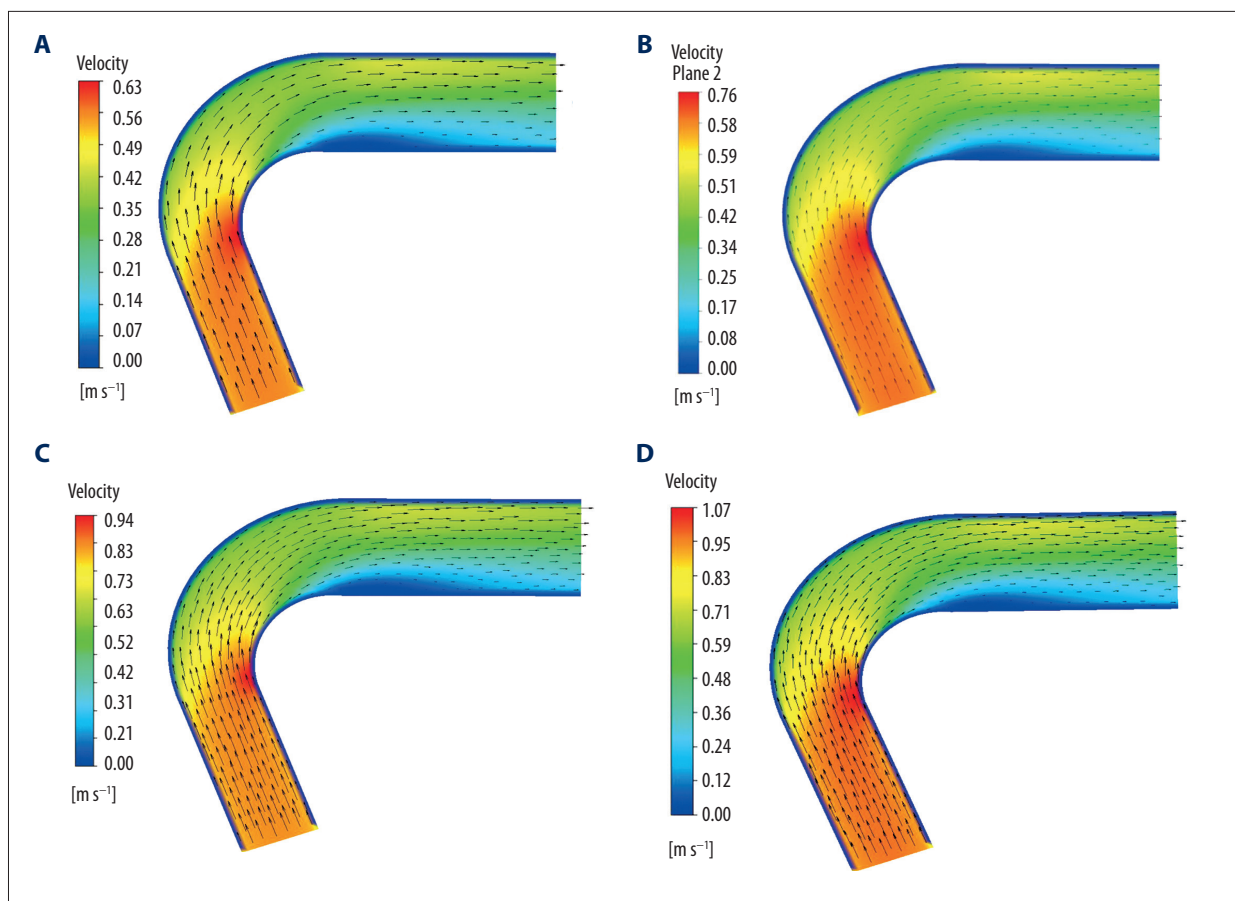


**Figure 6.** The calculated flow field in the inlet cannula. (A) at 4.0 lpm; (B) at 5.0 lpm; (C) at 6.0 lpm; (D) at 7.0 lpm.

connected to the pump. The low-velocity region was enlarged when the flow rate increased from 2.0 lpm to 3.0 lpm, but remained steady when the flow rate increased from 4.0 lpm to 7.0 lpm, and did not spread to the entrance of the blood pump. The existence of this slight low-velocity region should not have caused a thrombus in either the inlet cannula or the pump because the flow velocity was accelerated to a normal level. The CFD and PIV results show satisfactory agreement.

The limitations of this study are the methods used for CFD and PIV testing. Both CFD and PIV testing ignored the pulsatility of the blood flow and motion of the heart. The pulsatility of the flow affects the flow fields within the cannula; in particular, the amount of flow recirculation is likely to be increased as vortices are generated during the flow deceleration phase, possibly reducing the stagnant and low shear volumes. Compared with the PIV results, the CFD results showed a larger low-velocity flow region after the bent section of the inlet cannula because the boundary condition at the inlet cannula entrance was given as averaged distributed static pressure in the CFD simulation, but the actual boundary condition at the inlet cannula entrance is impossible to determine as average pressure.

In the future, the effects of various inlet cannula tip geometries and positions will be investigated with respect to potential thrombus formation within the blood pump and aorta.

### Conclusions

The simulation verified the optional bend characteristics of the soft silicone tube that can cause thrombi inside the axial blood pump. The cone-shaped bent inlet cannula reduced the risk of thrombus generation inside the LAP23 by eliminating the stagnant flow region. The PIV results showed the similar low-velocity region in the inlet cannula with the CFD results. In general, studying the inlet cannulas for the LAP23 can beneficially reduce the risk of thrombus generation in clinical practice.

Despite certain limitations, the effect of a cone-shaped inlet cannula on decreasing thrombus generation has been analyzed and verified by CFD and PIV technology.

## References:

1. Pennings KA, Tuijl SV, Vosse FNVD et al: Estimation of left ventricular pressure with the pump as "sensor" in patients with a continuous flow LVAD. *Int J Artif Organs*, 2015; 38(8): 433-43
2. Sheriff J, Girdhar G, Chiu WC et al: Comparative efficacy of in vitro and in vivo metabolized aspirin in the DeBakey ventricular assist device. *J Thromb Thrombolysis*, 2014; 37(4): 499-506
3. Tanoue Y, Jinzai Y, Tominaga R: Jarvik 2000 axial-flow ventricular assist device placement to a systemic morphologic right ventricle in congenitally corrected transposition of the great arteries. *J Artif Organs*, 2016; 19(1): 97-99
4. Tchanchaleishvili V, Hallinan W, Schwarz KQ et al: Long-term total cardiac support in a Fontan-type circulation with HeartMate II left ventricular assist device. *Interact Cardiovasc Thorac Surg*, 2016; 22(5): 692-94
5. Saeed D, Maxhera B, Albert A et al: Conservative approaches for HeartWare ventricular assist device pump thrombosis may improve the outcome compared with immediate surgical approaches. *Interact Cardiovasc Thorac Surg*, 2016; 23(1): 90-95
6. Fraser KH, Zhang T, Taskin ME et al: Computational fluid dynamics analysis of thrombosis potential in left ventricular assist device drainage cannulae. *ASAIO J*, 2010; 56(3): 157-63
7. Alexander T, Dimitar N, Vassil P: New technique for implantation of the inflow canula of Berlin heart INCOR system. *Eur J Cardio-Thorac Surg*, 2006; 30(4): 678-79
8. Komoda T, Weng Y, Hetzer R: Technique for insertion of the inflow cannula of the INCOR left ventricular assist device. *Ann Thorac Surg*, 2008; 85(4): 1466-67
9. Wieselthaler GM, Schima H, Wolner E: Special considerations on the implantation technique for the MicroMed-DeBakey ventricular assist device axial pump. *Ann Thorac Surg*, 2003; 76(6): 2109-11
10. Laumen M, Kaufmann T, Timms D et al: Flow analysis of ventricular assist device inflow and outflow cannula positioning using a naturally shaped ventricle and aortic branch. *Artif Organs*, 2010; 34(10): 798-806
11. Kapetanakis EI, Stamou SC, Dullum MK et al: The impact of aortic manipulation on neurologic outcomes after coronary artery bypass surgery: A risk-adjusted study. *Ann Thorac Surg*, 2004; 78(5): 1564-71
12. Schmid C, Jurmann M, Birnbaum D et al: Influence of inflow cannula length in axial-flow pumps on neurologic adverse event rate: Results from a multi-center analysis. *J Heart Lung Transplant*, 2008; 27(3): 253-60
13. Cohen DG, Thomas JD, Freed BH et al: Echocardiography and continuous-flow left ventricular assist devices: evidence and limitations. *JACC Heart Fail*, 2015; 3(7): 554-64
14. Zacharias M, Dhingra R: Percutaneous treatment of severe aortic insufficiency in a patient with left ventricular assist device. *JACC Cardiovasc Interv*, 2015; 8(5): 750-51
15. Fatullayev J, Samak M, Sabashnikov A et al: Continuous-flow left ventricular assist device thrombosis: A danger foreseen is a danger avoided. *Med Sci Monit Basic Res*, 2015; 21: 141-44
16. Yang XC, Zhang Y, Gui XM et al: Computational fluid dynamics-based hydraulic and hemolytic analyses of a novel left ventricular assist blood pump. *Artif Organs*, 2011; 35(10): 948-55
17. Untaroiu A, Wood HG, Allaire PE et al: Computational design and experimental testing of a novel axial flow LVAD. *ASAIO J*, 2005; 51(6): 702-10
18. Medvitz RB, Kreider JW, Manning KB et al: Development and validation of a computational fluid dynamics methodology for simulation of pulsatile left ventricular assist devices. *ASAIO J*, 2007; 53(2): 122-31
19. Zhang Y, Zhan Z, Gui XM et al: Design optimization of an axial blood pump with computational fluid dynamics. *ASAIO Journal*, 2008; 54(2): 150-55
20. Eckmann DM, Bowers S, Stecker M, Cheung AT: Hematocrit, volume expander, temperature, and shear rate effects on blood viscosity. *Anesth Analg*, 2000; 91(3): 539-45
21. Alison SC, Wu ZJ, Robert LK et al: Novel ventricular apical cannula: In vitro evaluation using transparent, compliant ventricular casts. *ASAIO J*, 1998; 44(5): 691-95